Sphere-to-Rod Transition in the Shape of Anionic Surfactant Micelles Determined by Surface Tension Measurements

R. G. Alargova,† K. D. Danov,† J. T. Petkov,† P. A. Kralchevsky,*,† G. Broze,‡ and A. Mehreteab§

Laboratory of Thermodynamics and Physico-chemical Hydrodynamics, Faculty of Chemistry, University of Sofia, 1126 Sofia, Bulgaria, Colgate-Palmolive Research and Development, Inc., Avenue Du Parc Industriel, B-4041 Milmort (Herstal), Belgium, and Colgate-Palmolive Company, Technology Center, 909 River Road, Piscataway, New Jersey 08854-5596

Received April 18, 1997. In Final Form: July 30, 1997⊗

We present experimental data showing that the surface tension, σ, of anionic surfactant (sodium dodecyl dioxyethylene sulfate: SDP-2S) solutions undergoes a substantial change in the vicinity of the transition from sphere to cylinder in the micelle shape. The formation of cylindrical (rodlike) micelles at relatively low surfactant concentrations (between 2 and 8 mM) is promoted by the presence of Al^{3+} ions in the solution. In the experiments we fixed the ionic strength of the added electrolyte but varied the molar fractions of NaCl and $AlCl_3$. We established that the observed variation of σ in a vicinity of the sphere-to-rod transition can be attributed to two competitive effects: (i) competition between Na^+ and Al^{3+} counterions for the adsorption in the subsurface Stern layer and (ii) competition between the solution surface and the surfaces of the micelles to adsorb the Al^{3+} counterions. The concentration of free Al^{3+} ions in the solution is substantially reduced due to binding of Al^{3+} to the micelles. The latter effect is studied experimentally by means of ultrafiltration experiments. We develop a theoretical model that allows us to calculate the true bulk (background) concentrations of Na^+ and Al^{3+} ions, and the variation of σ in the vicinity of the sphere-to-rod transition. Good agreement between theory and experiment is achieved. The results show that the transition from sphere to cylinder in the micelle shape can be detected from the plot of the surface tension vs the surfactant-to-Al^{3+} ratio. The paper also contains experimental data for the dependence of the CMC and surface tension of SDP-2S solutions on the ionic strength, which may represent independent interest.

1. Introduction

As known, the spherical surfactant micelles undergo a transition to larger rodlike aggregates with the increase of surfactant concentration.[1] It was established experimentally that the formation of rodlike micelles is enhanced by the addition of electrolyte and/or decreasing the temperature,[2−10] as well as by increasing the length of the surfactant hydrocarbon chain.[11−13] Note that the aforementioned experimental studies were performed using *monovalent* (1:1) electrolyte.

It was recently established[14] that the presence of multivalent counterions (Ca^{2+}, Al^{3+}) in solutions of anionic surfactant (sodium dodecyl dioxyethylene sulfate: SDP-2S) strongly enhances the formation of rodlike micelles. A qualitative explanation of this fact is that a multivalent counterion, e.g., Al^{3+}, can bind together three surfactant headgroups at the micelle surface, thus causing a decrease of the area per headgroup.[14] In accordance with the theory by Israelachvili et al.,[1,15] this will induce a transition from spherical to cylindrical micelles.

The experiment[14] shows that the formation of rodlike micelles in the presence of multivalent counterions differs from the micellization in the presence of 1:1 electrolyte in several aspects:

(i) The multivalent counterions are much more effective as promoters of the formation of rodlike micelles than the monovalent counterions. For example, at 8 mM surfactant concentration, the molar concentration of Na^+ needed to cause a transition from spherical to rodlike micelles is 230 times larger than the respective molar concentration of Al^{3+}.

(ii) In the presence of multivalent counterions cylindrical micelles (of aggregation number up to 4000) appear at relatively low surfactant concentration[14] (from 2 to 8 mM), corresponding to *isotropic* solutions. In other words, the average distance between the micelles is larger than the micelle average length and liquid-crystal-like ordering of micelles does not appear.

(iii) When the concentration of multivalent counterions is fixed and the surfactant concentration is varied, one observes cylindrical micelles at the *lower* surfactant concentrations and spherical micelles at the *higher* surfactant concentrations. This is exactly opposite to the

* To whom correspondence should be addressed.
† University of Sofia.
‡ Colgate-Palmolive Research and Development.
§ Colgate-Palmolive Co.
⊗ Abstract published in *Advance ACS Abstracts,* September 15, 1997.

(1) Israelachvili, J. N. *Intermolecular and Surface Forces*; Academic Press: London, 1991; Chapter 17.
(2) Mazer, N. A.; Benedek, G. B.; Carey, M. C. *J. Phys. Chem.* **1976**, *80,* 1075.
(3) Missel, P. J.; Mazer, N. A.; Benedek, G. B.; Young, C. Y.; Carey, M. C. *J. Phys. Chem.* **1980**, *84,* 1044.
(4) Hayashi, S.; Ikeda, S. *J. Phys. Chem.* **1980**, *84,* 744.
(5) Porte, G.; Appell, J.; Poggl, Y. *J. Phys. Chem.* **1980**, *84,* 3105.
(6) Porte, G.; Appell, J. *J. Phys. Chem.* **1981**, *85,* 2511.
(7) Hoffmann, H.; Klaus, J.; Thurn, H.; Ibel, K. *Ber. Bunsen-Ges. Phys. Chem.* **1983,** *87,* 1120.
(8) Chen, J.-M.; Su, T. M.; Mou, C. Y. *J. Phys. Chem.* **1986**, *90,* 2418.
(9) Missel, P. J.; Mazer, N. A.; Carey, M. C.; Benedek, G. B. *J. Phys. Chem.* **1989**, *93,* 8354.
(10) Lin, T.-L.; Tseng, M.-Y.; Chen, S.-H.; Roberts, M. F. *J. Phys. Chem.* **1990**, *94,* 7239.
(11) Tausk, R.; Overbeek, J. Th.G. *Colloid Interface Sci.* **1976**, *2,* 379.
(12) Nicoli, D. F.; Dawson, D. R.; Offen, J. W. *Chem. Phys. Lett.* **1979,** *66,* 291.
(13) Missel, P. J.; Mazer, N. A.; Benedek, G. B.; Carey, C. *J. Phys. Chem.* **1983**, *87,* 1264.
(14) Alargova, R.; Petkov, J.; Petsev, D.; Ivanov, I. B.; Broze, G.; Mehreteab, A. *Langmuir* **1995**, *11,* 1530.
(15) Israelachvili, J. N.; Mitchell, D. J.; Ninham, B. W. *J. Chem. Soc., Faraday Trans. 2* **1976,** *72,* 1525.

S0743-7463(97)00399-5 CCC: $14.00 © 1997 American Chemical Society

case when electrolyte is not added. The explanation is that the transition from sphere to rod occurs at a *given ratio of surfactant to electrolyte*; in the excess of electrolyte, cylindrical micelles are formed, whereas in the excess of surfactant, the micelles are spherical.[14] For the sake of brevity we term the transitional value of the surfactant-to-electrolyte ratio the "critical ratio".

In the present study we investigate experimentally the behavior of the surface tension in the vicinity of the critical ratio. We will mention in advance that the surface tension, σ, turns out to be sensitive to the sphere-to-rod transition, and consequently, σ can be used as an indicator of such a transition.

In the next section we describe the experimental conditions and the results from the measurements of micelle size and surface tension. As the surfactant micelles adsorb Al^{3+} ions and thus substantially affect the ionic strength of solution, we carried out ultrafiltration experiments to determine the background concentration of Al^{3+} in the solution.

In section 3 we present a quantitative interpretation of the ultrafiltration experiments and derive equations for calculating the true values of the separate ionic concentrations and the ionic strength. On the basis of these results, in section 4 we quantitatively interpret the observed changes of the surface tension in the vicinity of the critical ratio.

2. Experimental Part

2.1. Solutes and Solutions. The surfactant used in the present work is sodium dodecyl dioxyethylene sulfate (SDP-2S), Empicol ESB70, Wilson Co., England with structure $CH_3(CH_2)_{11}(OC_2H_4)_2OSO_3Na$. The ionic strength is due to a mixture of NaCl and $AlCl_3 \cdot 6H_2O$ (Sigma). All micellar solutions were prepared by using deionized water (Milli-Q, Organex grade). The temperature in surface tension measurements was 27 ± 0.1 °C, while in the ultrafiltration experiments it was slightly lower, 25 ± 0.1 °C.

It may seem questionable whether the Al^{3+} ions exist in the solutions in trivalent form or if some complexes with the OH^- ions are formed. It is known that below pH = 4.0 the dissolved Al is present mostly in the form of trivalent ions.[16−18] In our case the dissolved $AlCl_3$ decreases the pH of the solutions down to about 3.0−3.5 and our estimates based on the data[17,18] about the stability of the various compounds, $Al(OH)^{2+}$, $Al(OH)_2^+$, and $Al(OH)_3$, showed that the fraction of Al^{3+} is above 98% at pH = 3.0 and above 95% at pH = 3.5.

We determined the critical micellization concentration (CMC) of SDP-2S by measuring the average intensity of the scattered light (static light scattering) as a function of surfactant concentration. The appearance of micelles leads to a break point in the concentration dependence, after which the intensity of the scattered light increases linearly with the micellar concentration. As we did not find literature data about the dependence of CMC of SDP-2S on the ionic strength of solution, I, we did the respective measurements. We established experimentally that ln(CMC) decreases linearly with ln I in the concentration range $0.024 < I < 0.128$ M:

$$\ln \mathrm{CMC} = -11.444 - 0.7573 \ln I \qquad (2.1)$$

Similar dependence has been experimentally established for other surfactants.[19] To obtain the dependence 2.1, we varied I by addition of NaCl.

Further, we checked whether CMC of SDP-2S depends on the molar fraction of NaCl and $AlCl_3$ at a fixed value of the total ionic strength, I. The results for $I = 0.024$ and 0.012 M are shown in

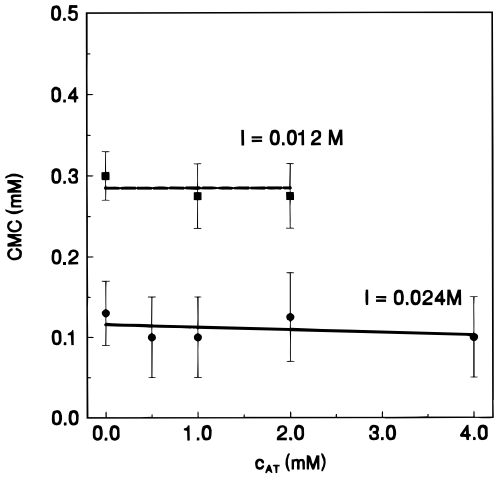

Figure 1. Critical micellization concentration (CMC) of SDP-2S, measured with static light scattering, vs the total Al^{3+} counterions concentration, c_{AT}, at two ionic strengths $I = 0.012$ and $I = 0.024$ M. The ionic strength is maintained by a mixture of $AlCl_3$ and NaCl.

Figure 1. The end points on the left and on the right correspond to solutions of pure NaCl and $AlCl_3$, respectively, whereas the intermediate points are measured with mixtures of these two salts at a fixed ionic strength. One can see that the CMC depends mostly on the total ionic strength and rather weakly on the specific type of the dissolved microions, which is consonant with the results of other studies.[20,21] For low surfactant concentrations (in the vicinity of the CMC and lower), the presence of Al^{3+} causes some precipitation of the surfactant, which decreases the accuracy of the light scattering results for CMC. To verify the results, we obtained independent data for CMC by measuring the surface tension isotherms of SDP-2S in the presence of NaCl and $AlCl_3$ at $I = 0.024$ M. We determined a CMC of about 1×10^{-4} M for SDP-2S, which is close to the value obtained by the static light scattering experiments, the lower curve in Figure 1.

In our studies on the growth of rodlike micelles of SDP-2S (see below), we fixed the ionic strength of the added electrolyte, $I =$ 0.024 M, but varied the molar fractions of NaCl and $AlCl_3$.

2.2. Dynamic Light Scattering Experiments. The light scattering experiments were performed by means of an Autosizer 4700C (Malvern, England) supplied with argon laser (Innova, Coherent), operating at wavelength 488 nm, and a K7032 CE 8-Multibit 128-channel correlator. We determined the diffusion coefficient of SDP-2S micelles and studied its concentration dependence by using the dynamic light scattering method. The surfactant concentration used was varied from 2 to 60 mM; in other words, it is low enough to avoid multiple light scattering from the micelles. The temperature in all measurements was maintained at 27 ± 0.1 °C.

In ref 14 we established experimentally that an important parameter characterizing the transition from spherical to rodlike micelles is the surfactant to multivalent counterion ratio defined as follows:

$$\xi = c_{SM}/(3c_{AT}) \qquad c_{SM} \equiv c_S - \mathrm{CMC(I)} \qquad (2.2)$$

where c_{SM} is the molar concentration of surfactant molecules in micellar form, c_{AT} is the average total molar concentration of the Al^{3+} counterion in the solution, c_S is the total surfactant concentration. In other words, ξ equals the ratio of the net charge of the micellar ionizable groups to the net charge of the dissolved multivalent counterions (Al^{3+}). It was established in ref 14 that in the presence of Al^{3+} the variation of ξ has a dramatic effect on the size of the micelles; for instance, a decrease of ξ from 1.2 to 0.67 leads to a 60 times increase of the mean mass aggregation number of the micelles.

From the measured micelle diffusion coefficient, D, an *apparent* hydrodynamic radius of the micelles, R_h, was calculated by means of the known Stokes−Einstein formula, $R_h = kT/(6\pi\eta D)$, where

(16) Marchenko, Z. *Photometric Determination of the Elements;* Mir: Moscow, 1971 (in Russian).
(17) Lurie, Y. Y. *Handbook of Analytical Chemistry;* Khimia: Moscow, 1989 (in Russian).
(18) Bontchev, P. *Introduction to Analytical Chemistry;* Nauka i Izkustvo: Sofia, 1985 (in Bulgarian).
(19) Hunter, R. J. *Foundations of Colloid Science*; Clarendon Press: Oxford, U.K., 1987.
(20) Tanford, C. *The Hydrophobic Effect: Formation of Micelles and Biological Membranes;* Wiley: New York, 1980; Chapter 7.
(21) Oko, M. U.; Venable, R. L. *J. Colloid Interface Sci.* **1971**, *35*, 53.

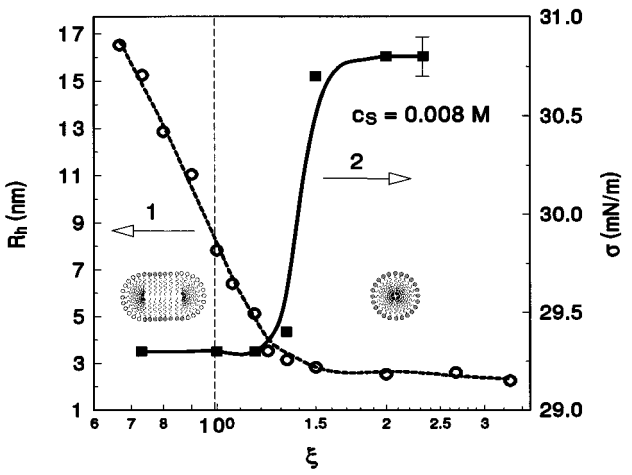

Figure 2. Apparent hydrodynamic radius of micelles, R_h, (curve 1), and surface tension, σ (curve 2), as a function of $\xi = c_{SM}/(3c_{AT})$ at $I = 0.024$ M. The total surfactant concentration is constant $c_S = 0.008$ M. The parameter ξ is varying, changing the total concentration of Al^{3+}.

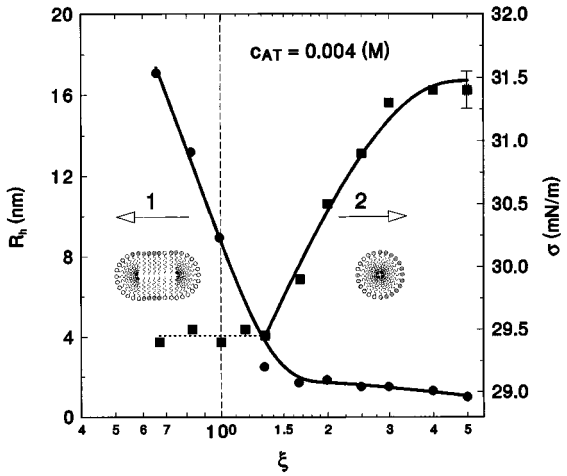

Figure 3. Apparent hydrodynamic radius of micelles, R_h (curve 1), and surface tension, σ (curve 2), as a function of $\xi = c_{SM}/(3c_{AT})$ at $I = 0.024$ M. The total concentration of Al^{3+} counterions is constant, 0.004 M. The parameter ξ is varying with an increase in the surfactant concentration c_S. The solid line (curve 2) presents the theoretical fit of the data according to eq 4.7.

k is the Boltzmann constant, T is the temperature, and η is the viscosity of the solvent. R_h coincides with the *real* hydrodynamic radius of the micelles only when they are spherical. In Figures 2−4 we present experimental data for R_h; part of the experimental points are taken from ref 14, and others represent new measurements.

Figure 2 shows data for R_h vs ξ for fixed total surfactant concentration, $c_S = 8$ mM. For the larger values of ξ the SDP-2S micelles are small and spherical, whereas for the smaller ξ a rapid increase in the micelle size is observed, which indicates the growth of rodlike (cylindrical) micelles.[14] One sees that the transition from sphere to cylinder in the micelle shape happens close to the value $\xi = 1$. This means that an Al^{3+} ion binds together three surfactant headgroups at the micelle surface, thus causing a decrease of the area per headgroup.[14] As already mentioned, in accordance with the theory by Israelachvili et al.,[1,15] the increase of the area per headgroup induces a transition from spherical to cylindrical micelles.

As mentioned earlier, in ref 14 it was established that the latter transition depends on the value of the ratio ξ, but not on the values of c_{SM} and c_{AT} separately, cf. eq 2.2. In fact, we term the transitional value of ξ the "critical ratio". A similar transitional value of ξ is present also for solutions containing Ca^{2+} (instead of Al^{3+}) ions.[14]

2.3. Surface Tension Measurements. As is well-known, the plot of surface tension, σ, vs the surfactant concentration exhibits a break at the CMC. We decided to verify whether such a break happens in the vicinity of the critical ratio (the second CMC) as well. For that purpose we measured the surface tension of the investigated solutions by means of a Krüss tensiometer with the Wilhelmy plate method at 27 ± 0.1 °C.

Indeed, we observed an abrupt change in the surface tension, σ, in the vicinity of the critical ratio; see the second curve in Figure 2. The surface tension turns out to be higher in the region of the spherical micelles and lower in the region of the cylindrical micelles. As established in the theoretical part of this study (see below), this lowering of σ can be attributed to the adsorption of Al^{3+} ions in the subsurface layer of the solution (the Stern layer). Indeed, the smaller ξ values correspond to larger Al^{3+} concentrations; cf. eq 2.2. Note that the data in Figure 2 are obtained by variation of ξ through altering of Al^{3+} concentration at a fixed total surfactant concentration, $c_S = 8$ mM.

Our experimental data for the supplementary case, when ξ is varied by altering the total surfactant concentration at fixed Al^{3+} concentration in the solutions, $c_{AT} = 4$ mM, are shown in Figure 3. One sees that (similar to Figure 2) the critical ratio is close to the point $\xi = 1$, where the surface tension, σ, undergoes a pronounced change in its value. Again, σ is higher in the region of the spherical micelles and lower in the region of the cylindrical micelles (Figure 3).

Finally, we conducted a third type of experiment: we fixed the surfactant-to-aluminum ratio, ξ, but varied proportionally the surfactant and aluminum concentration. Experimentally, this

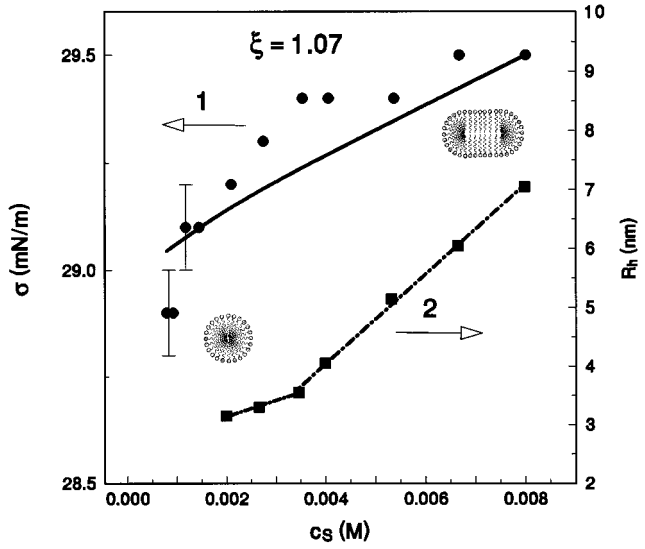

Figure 4. Apparent hydrodynamic radius of micelles, R_h (curve 1), and surface tension, σ (curve 2), as a function of surfactant concentration, c_S, at $I = 0.024$ M. The parameter $\xi = 1.07$ is constant.

was realized by simply diluting an initial solution with an aqueous solution of NaCl with the same ionic strength, $I = 24$ mM. The results are presented in Figure 4. One sees that growth of cylindrical micelles happens at the higher surfactant concentrations, c_S, whereas the micelles are small and spherical for the lower c_S. The data for the surface tension, σ, of these solutions are quite intriguing. First, one observes that σ increases with the increase of the surfactant concentration, which is a tendency opposite to our common physical insight. Second, σ is higher for the solutions with cylindrical micelles and lower for the solutions with spherical micelles, which is exactly opposite to the tendency exhibited by the data in Figures 2 and 3.

This interesting behavior of the surface tension of the investigated solutions stimulated us for a theoretical study of the observed phenomena (see below). One may anticipate that the latter are related (at least) to two competitive effects: (i) competition between Na^+ and Al^{3+} counterions for the adsorption in the subsurface Stern layer and (ii) competition between the solution surface and the surfaces of the micelles to adsorb the multivalent Al^{3+} counterions. The situation is additionally complicated by the fact that the concentration of Al^{3+} is comparable with the surfactant concentration, and consequently, the concentration of free Al^{3+} might be substantially reduced due to adsorption of Al^{3+} on the surface of the micelles. The latter effect was studied experimentally by means of the ultrafiltration experiments described below.

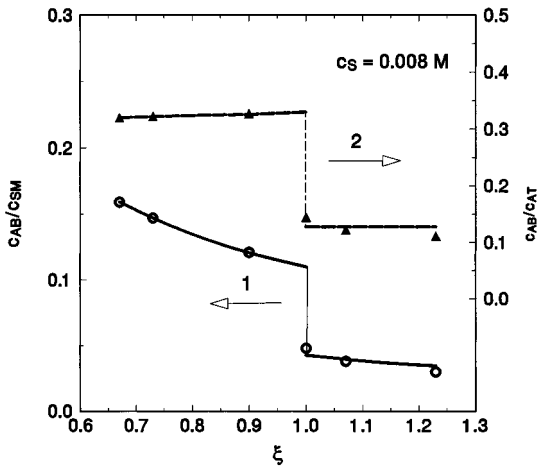

Figure 5. Plots of ultrafiltration data for c_{AB}/c_{SM} (curve 1) and c_{AB}/c_{AT} (curve 2) vs ξ for fixed $c_S = 0.008$ M and $I = 0.024$ M in the presence of Al^{3+} and Na^+. The lines are drawn by means of eqs 3.9 and 3.10.

2.4. Ultrafiltration Experiments. As known, the multivalent counterions bind strongly to the negatively charged surface of the anionic micelles and can be removed from the solution by performing an ultrafiltration experiment using a membrane with appropriate pore size.[22,23] When the micelles are rejected by an efficient ultrafiltration membrane, all ions belonging to the Stern and diffuse electric double layers around the micelles are retained and the counterion concentration in the solution permeating through the pores is identical to that of the surrounding aqueous medium.

We applied this method to determine the background concentration of the unbound Al^{3+} counterions, c_{AB}, in solutions containing 8 mM SDP-2S at ionic strength $I = 24$ mM (calculated using the concentrations of the added electrolytes) and at different values of the total input concentration of Al^{3+}, c_{AT}. The ultrafiltration experiments were carried out at room temperature (25 ± 2 °C) in dead-end mode in a 100 mL stirred cell. The transmembrane pressure was kept constant at 0.5 atm during the experiments. We used a polysulfonic membrane with molecular weight cutoff 6000, which is small enough to permit the retention of the smallest SDP-2S micelles. The cell was initially filled with 50 mL of the solution, and samples of 5 mL were taken throughout the run and then used for the spectrophotometric determination of the Al^{3+} concentration in the permeate, c_{AB}. For that purpose we used a color reaction between the ammonium salt of the aurintricarboxylic acid (Aluminon, Sigma) and the Al^{3+} ions taking place at low pH values.[16]

In Figure 5 we plot the experimental data for c_{AB}/c_{SM} and c_{AB}/c_{AT} vs ξ for $c_S = 8$ mM, where $c_{SM} = c_S - CMC$ is the average concentration of the surfactant built in the micelles and c_S is the total surfactant concentration. The ratio c_{AB}/c_{AT} expresses the part of the aluminum ions that are not associated with the micelles; one sees in Figure 5 that this part decreases from 32% to 11% with the increase of ξ. In other words the predominant part of the Al^{3+} ions in the investigated solutions (from 68% to 89%) is associated with the surfactant micelles. In this aspect there is a great difference in the micelle growth in solutions of 1:1 electrolyte, when the amount of counterions associated with the micelles is negligible.[3,9] To be able to interpret the data in the case when Al^{3+} ions are present, we need to know what is the aluminum background concentration, c_{AB}, corresponding to a given total aluminum concentration c_{AT}. To obtain such an estimate, we use theoretical considerations presented below.

3. Interpretation of the Ultrafiltration Data

3.1. Calculation of the True Ionic Strength of the Micellar Solution. The binding of Al^{3+} ions to the micelles is accompanied by release of Na^+ ions from the micelles. Consequently, the true background ionic strength of the solution, I_t, differs from the calculated ionic strength, I, of the electrolyte (NaCl + $AlCl_3$) added to the solution. The background concentration of the Na^+ ions, c_{NB}, can be calculated by means of the following expression:

$$c_{NB} = c_{NT} + 3(c_{AT} - c_{AB}) + [c_S - CMC - 3(c_{AT} - c_{AB})]\alpha_{Na} + CMC \quad (3.1)$$

Here c_{NT} expresses the total input concentration of Na^+ from the added NaCl; the term $3(c_{AT} - c_{AB})$ stands for the Na^+ counterions replaced from the micelles by adsorbed Al^{3+} ions; the next term, $[c_S - CMC - 3(c_{AT} - c_{AB})]\alpha_{Na}$, accounts for the Na^+ ions dissociated from the micelle headgroups, which are not occupied by adsorbed Al^{3+}; α_{Na} denotes the degree of dissociation of the micelle headgroups free of adsorbed Al^{3+} ($0 < \alpha_{Na} < 1$); the fact that α_{Na} can be less than 1 accounts for a possible adsorption of Na^+ in the micelle Stern layer; finally, the term CMC in eq 3.1 accounts for the Na^+ ions dissociated from the free surfactant monomers in the solution.

Next, the true background ionic strength of the solution reads

$$I_t = \frac{1}{2}[9c_{AB} + c_{NB} + (3c_{NT}) + CMC] \quad (3.2)$$

The term in parentheses expresses the concentration of the Cl^- ions dissociated from the dissolved $AlCl_3$ and NaCl, and the last term in eq 3.2 accounts for the surfactant monomers in the solution. The combination of eqs 3.1 and 3.2 yields

$$I_t = 3c_{AB} + 3c_{AT} + c_{NT} + CMC + \frac{1}{2}(c_S - CMC - 3c_{AT} + 3c_{AB})\alpha_{Na} \quad (3,3)$$

3.2. Calculation of the Background Concentration of Aluminum, c_{AB}. The total Al^{3+} concentration in the solution can be expressed in the form

$$c_{AT} = c_{AB} + (N_D + N_{St})c_M \qquad c_M = c_{SM}/M \quad (3.4)$$

where N_D and N_{St} are the number of Al^{3+} ions contained in the diffuse and Stern parts of the electric double layer of a micelle; c_M is the concentration of the micelles, whose average aggregation number is denoted by M. To estimate N_D, we will use the linearized Poisson−Boltzmann equation for the electric potential, ψ, around a spherical micelle:

$$\frac{1}{r^2}\frac{d}{dr}\left(r^2\frac{d\psi}{dr}\right) = \kappa^2\psi \qquad \kappa^2 \equiv \frac{8\pi e^2 I_t}{\epsilon kT} \quad (3.5)$$

Here r is the radial coordinate, κ^{-1} is the Debye length, e is the electronic charge, and ϵ is the dielectric permittivity of water. The boundary condition for eq 3.5 reads

$$\frac{d\psi}{dr}\Big|_{r=r_M} = -\frac{e\alpha M}{\epsilon r_M^2} \quad (3.6)$$

where r_M is the micelle radius and α is the fraction of the micelle headgroups, whose counterions belong to the *diffuse* double electric layer around the micelle. Further, one can calculate N_D by using the Boltzmann formula:

$$N_D = c_{AB}\int_{r_M}^{\infty}\left[\exp\left(-\frac{3e\psi}{\epsilon kT}\right) - 1\right]4\pi r^2\, dr \quad (3.7)$$

A linearization of the exponent in eq 3.7, along with eqs 3.5 and 3.6, allows us to take the integral; the result reads

(22) Scamehorn, J. F.; Christian, S. D.; Ellington, R. T. In *Surfactant Based Separation Processes;* Scamehorn, J. F., Harwell, T. H. Eds.; M. Dekker: New York, 1989.

(23) Hafiane, A.; Issid, I.; Lemorandt, D. *J. Colloid Interface Sci.* **1991**, *142*, 167.

$$\frac{N_D}{M} = \frac{3c_{AB}}{2I_t}\alpha \qquad (3.8)$$

Note that we obtained eq 3.8 for the limiting case of small spherical micelles. One can check that in the other limit of infinitely long cylindrical micelles exactly the same expression for N_D/M holds. Hence, one may use eq 3.8 for both spherical and cylindrical micelles. In addition, one realizes that $N_{St} = (1 - \alpha)M$. After substitution of the last equation and eq 3.8 into eq 3.4 one obtains

$$\frac{c_{SM}}{3\xi} = c_{AB} + \left[\frac{3\alpha c_{AB}}{2I_t} + (1 - \alpha)\right](c_S - \mathrm{CMC}) \qquad (3.9)$$

see also eq 2.2. To determine independently c_{AB} and α as functions of ξ, one needs one more equation, in addition to eq 3.9. This equation is to be an isotherm for the adsorption of Al^{3+} in the micelle Stern layer. We tried the Langmuir and Volmer adsorption isotherms, but they compared unsatisfactorily with the experiment. In contrast, it turned out that the Henry adsorption isotherm,

$$1 - \alpha = \begin{cases} 3c_{AB}/H_1 & \text{for } \xi < 1 \\ 3c_{AB}/H_2 & \text{for } \xi > 1 \end{cases} \qquad (3.10)$$

compares very well with the experimental data; here, H_1 and H_2 are the coefficients of Henry, which determine the adsorption of Al^{3+} on the surface of cylindrical and spherical micelles, respectively. We determined H_1 and H_2 as adjustable parameters. For that purpose we fitted the plot of c_{AB}/c_{SM} vs ξ in Figure 5; the theoretical values of c_{AB} were obtained by numerically solving eq 3.9, along with eq 3.10, for each value of ξ. The best fit is shown in Figure 5 with the solid line. The values of the adjustable parameters thus determined are

$$H_1 = 1.64 \times 10^{-3}\ \mathrm{M} \qquad H_2 = 4.07 \times 10^{-4}\ \mathrm{M} \qquad (3.11)$$

It should be noted that when solving eqs 3.9−3.10, we take into account the dependence of CMC on the true ionic strength, I_t; cf. eqs 1.1 and 3.3. On the other hand, the values of c_{SM} and ξ are *defined* through the value CMC corresponding to the apparent ionic strength, $I = 0.024$ M, of the electrolyte (NaCl and $AlCl_3$) added to the solution; that is why the values of c_{SM} and ξ do not vary with I_t. Detailed description of the procedure of calculations is given in the Appendix.

Equations 3.9 and 3.10 allow us to calculate the background Al^{3+} concentration, c_{AB}, as a function of the bulk surfactant and aluminum concentrations (and their combination ξ as well); these equations will be utilized below for the interpretation of the data for the surface tension (see Figures 2−4).

4. Interpretation of the Surface Tension Data

4.1. Adsorption of Na^+ and Al^{3+} in the Stern Layer. In the case of adsorption of an ionic surfactant from solution, the Gibbs adsorption equation can be expressed in two alternative but equivalent forms:[24]

$$d\sigma = -kT\sum_i \Gamma_i\, d\ln c_i \qquad (4.1)$$

$$d\sigma = -kT\sum_i \Gamma_i\, d\ln c_i^{(s)} + \sigma_{ch}\, d\psi_s \qquad (4.2)$$

(T = const). Here c_i and $c_i^{(s)}$ are the bulk and subsurface concentrations of the dissolved species and Γ_i are their adsorptions ($i = 1, 2, ...$); σ_{ch} and ψ_s are the surface charge density and surface potential. Equations 4.1 and 4.2 are equivalent because of the known relationships

$$c_i^{(s)} = c_i \exp\left(-\frac{Z_i e\psi_s}{kT}\right) \qquad \sigma_{ch} = \sum_i Z_i e\Gamma_i \qquad (4.3)$$

where Z_i denotes the valence of the ith species. The summation is carried out over all species, including the surfactant ions and the counterions.

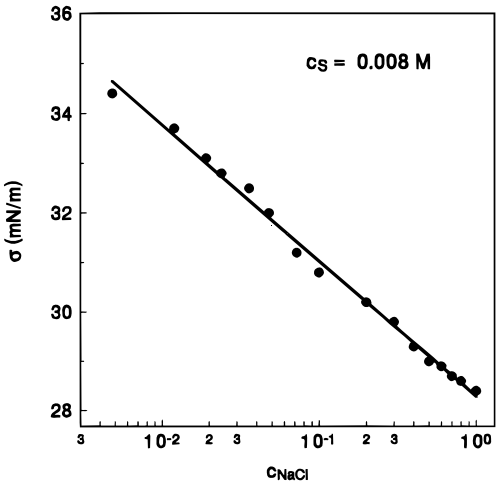

Figure 6. Surface tension, σ, of SDP-2S micellar solutions as a function of NaCl concentration. The total surfactant concentration is the same in all points, $c_s = 0.008$ M.

For the interpretation of the experimental data we will employ eq 4.1. It allows us to describe the adsorption of surfactant ions and counterions without explicitly taking into account the existence of a double electric layer. First we decided to check how this approach works with SDP-2S adsorption monolayers in the presence of NaCl only (without added $AlCl_3$). In Figure 6 we plotted the measured surface tension, σ, vs. the log of the NaCl concentration; the total surfactant concentration in this experiment was kept constant, $c_s = 8$ mM. One sees that the data complies very well with a straight line. Let us now apply eq 4.1 to interpret the data in Figure 6. As the CMC is rather low compared with the NaCl concentration, the latter practically coincides with the ionic strength of the solution, I. Then, eq 4.1 can be transformed to read

$$\frac{d\sigma}{d\ln I} = -kT\Gamma_s\left(\frac{d\ln \mathrm{CMC}}{d\ln I} + \theta_N\right) \qquad \theta_N \equiv \Gamma_N/\Gamma_s \qquad (4.4)$$

where Γ_s and Γ_N are the adsorptions of surfactant and Na^+ and θ_N is the degree of filling of the Stern layer with Na^+ ions. With the help of eq 2.1, one can estimate the derivative in the right-hand side of eq 4.4. Note that the two terms in parentheses in eq 4.4 have opposite signs, which is related to the fact that the adsorption of Na^+ in the Stern layer tends to decrease σ, whereas the decrease of CMC tends to increase σ. With $1/\Gamma_s = 50$ Å^2 from the slope of the line in Figure 6 one calculates $\theta_N = 0.86$; in other words, 86% of the Na^+ counterions belong to the Stern layer, and only 14% of them belong to the diffuse electric double layer. Note that in the above interpretation of the data in Figure 6 we have assumed that Γ_s = const, which is an often used assumption for surfactant concentration around and above the CMC.

In the case when both Na^+ and Al^{3+} ions are present in the solution, they will compete with each other for the adsorption in the Stern layer. To describe this effect, we

(24) Davis, J. T.; Riedal, E. K. *Interfacial Phenomena*; Academic Press: New York and London, 1963.

will use the Langmuir adsorption isotherm:

$$\theta_N = \frac{b_N c_{NB}}{1 + b_N c_{NB} + b_A c_{AB}} \qquad \theta_A \equiv \frac{3\Gamma_A}{\Gamma_s} = \frac{b_A c_{AB}}{1 + b_N c_{NB} + b_A c_{AB}} \quad (4.5)$$

where, as usual, c_{NB} and c_{AB} are the bulk (background) concentrations of Na^+ and Al^{3+}; the coefficients

$$b_N = \frac{\delta_N}{\Gamma_s} \exp\left(\frac{\Phi_N}{kT}\right) \qquad b_A = \frac{\delta_A}{\Gamma_s} \exp\left(\frac{\Phi_A}{kT}\right) \quad (4.6)$$

are related to the energy of adsorption, Φ_N or Φ_A, of an Na^+ or Al^{3+} ion in the Stern layer; the parameters δ_N and δ_A can be identified with the diameters of the respective hydrated ions. Below we use the values $\delta_N = 7.2$ Å and $\delta_A = 9.6$ Å; see, e.g., ref 1. The adsorption energies Φ_N and Φ_A will be determined from the experimental data as adjustable parameters.

4.2. Numerical Results and Discussion. To interpret the data for the surface tension, σ, in Figures 2−4, we integrate numerically the equation

$$d\sigma = -kT\Gamma_s\left(d \ln \mathrm{CMC} + \theta_N\, d \ln c_{NB} + \frac{\theta_A}{3} d \ln c_{AB}\right) \quad (4.7)$$

which stems from eq 4.1; θ_N and θ_A are given by eq 4.5, and CMC is determined as a function of the ionic strength by eq 2.1. The procedure of calculation is described in the Appendix. Here we should note that only one of the three differentials in the right-hand side of eq 4.7 is independent.

For the data in Figure 3 the independent parameter is ξ; the total aluminum concentration is fixed, $c_{AT} = 4$ mM. Then the total concentration of the added NaCl is determined from the condition for a fixed value of the ionic strength of the total added electrolyte:

$$c_{NT} + 6c_{AT} = I \equiv \mathrm{const} \quad (4.8)$$

We recall that in all experiments of surface tension measurement (except that related to Figure 6) the total ionic strength of the added electrolyte was one and the same, $I = 24$ mM. Next we determine c_{AB} from eqs 3.9−3.11, c_{NB} from eq 3.1, the true ionic strength, I_t, from eq 3.2, and CMC(I_t) from eq 2.1. As a boundary condition needed to start the integration of eq 4.7, we used the experimental point after which the surface tension starts increasing with ξ (Figure 3): $\xi = 1.33$, $\sigma = 29.45$ mN/m. The best fit for the data σ vs ξ is shown in Figure 3 with the full line; it corresponds to the following values of the adjustable parameters: $\Phi_N = 8.1kT$, $\Phi_A = 13.1kT$, and $\alpha_{Na} = 0.5$; cf. eq 3.1. The fact that $\Phi_N < \Phi_A$ is consonant with the greater charge of the Al^{3+} ion.

The above values of Φ_N and Φ_A call for some discussion. We tried to fit the experimental data with both eqs 4.1 and 4.2 (the latter combined with appropriate expressions from the double-layer theory for the regime of surface charge regulation). We found that eq 4.1 gives a better fit than eq 4.2. Physically, this means that the experimental data agree with a regime of fixed surface potential, ψ_s, rather than with surface charge regulation. This is not surprising: the experiment shows that often the surface potential is constant, i.e., independent of the electrolyte concentration; see, e.g., ref 25. In view of eqs 4.3 and 4.5 one can write

(25) Petsev, D. N.; Denkov, N. D. *J. Colloid Interface Sci.* **1992**, *149*, 329.

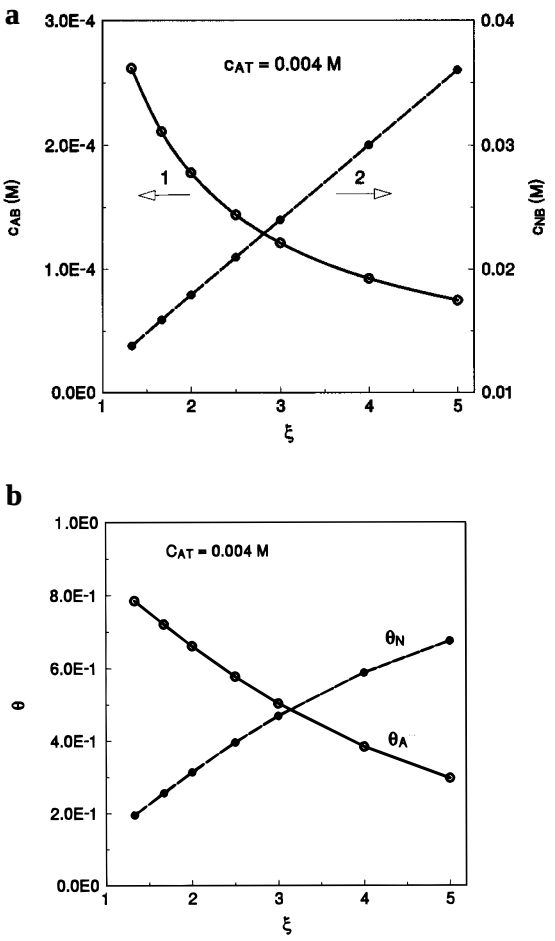

Figure 7. (a) Calculated values of c_{AB} (curve 1) and c_{NB} (curve 2) corresponding to the variation of the surface tension, σ, in Figure 3. The total aluminum counterman concentration is constant, $c_{AT} = 0.004$ M. (b) Calculated values of degrees of filling of the subsurface Stern layer with Al^{3+} and Na^+ counterions (cf. eq 4.5) corresponding to the variation of the surface tension, σ, in Figure 3. The total aluminum counterion concentration is constant, $c_{AT} = 0.004$ M.

$$\Phi_N = e\psi_s + \Phi_N^s \qquad \Phi_A = |3e\psi_s| + \Phi_A^s$$

where $|e\psi_s|$ accounts for the (mean field) electrostatic potential energy of the ion in the Stern layer and Φ_N^s and Φ_A^s express specific adsorption energies. The calculations based on the standard double-layer theory give $\psi_s = -19.5$ mV, $|e\psi_s| = 0.8\ kT$, $\Phi_N^s = 7.3\ kT$, and $\Phi_A^s = 10.7\ kT$. The comparatively low value of the work $|e\psi_s|$ of bringing of an ion from infinity to the Stern layer is due to the fact that the surface charge density is relatively low: more than 90% of the surface ionizable groups are neutralized by the counterions of the Stern layer.

Figure 7a shows the calculated values of c_{NB} and c_{AB}, corresponding to the variation of σ in Figure 3. One sees that the increase of ξ leads to decreasing of c_{AB} but increasing of c_{NB}. This is quite understandable, because at fixed c_{AT} the value of ξ is increased by increasing c_{SM} (cf. eq 2.2), which leads to the formation of new micelles; the latter adsorb additional Al^{3+} ions from the bulk and release Na^+ counterions in the bulk. Further, the adsorption of Al^{3+} and Na^+ counterions at the surface of the *solution* follows the same tendency as the bulk concentrations of the respective ions: see Figure 7b, which shows the calculated values of the degrees of filling of the subsurface Stern layer with Al^{3+} and Na^+ counterions, θ_A and θ_N cf. eq 4.5. As the adsorption energy of the Al^{3+} ions is greater ($\Phi_A > \Phi_N$), the decrease of θ_A (the desorption of Al^{3+} ions) has a stronger effect on the surface tension, σ, and causes its increase with increase of ξ (Figure 3).

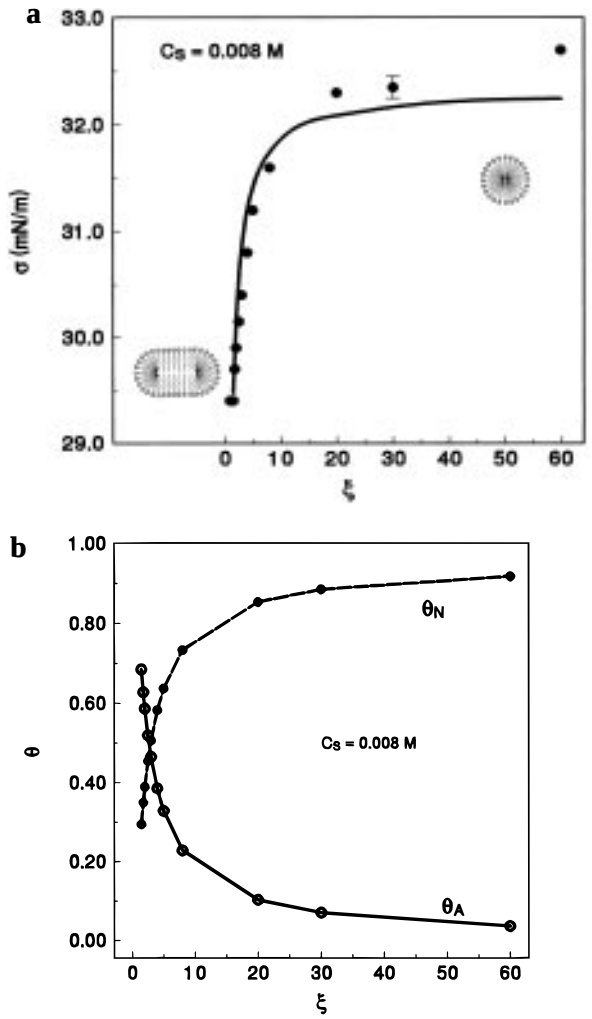

Figure 8. (a) Surface tension, σ, as a function of ξ at $I = 0.024$ M. The total surfactant concentration is constant, $c_S = 0.008$ M. The solid line presents the theoretical fit of the experimental data. (b) Calculated values of degrees of filling of the subsurface Stern layer with Al^{3+} and Na^+ counterions (cf. eq 4.5) corresponding to the variation of the surface tension, σ, in Figure 8a. The total surfactant concentration is constant, $c_S = 0.008$ M.

Let us now interpret the data for σ vs ξ in Figure 2, which are obtained at a fixed value of the total surfactant concentration, $c_S = 8$ mM and, as usual, $I = 24$ mM. This time ξ is increased by decreasing c_{AT}; see eq 2.2. Experimentally, this is achieved by diluting the initial solution the addition of solution containing $c_S = 8$ mM, $c_{NaCl} = 24$ mM, but without any $AlCl_3$. This procedure allows us to achieve comparatively high values of ξ. Figure 8a contains the data for σ vs ξ from Figure 2, together with additional data up to $\xi = 60$. The theoretical curve in Figure 8a is drawn with the parameter values determined from the fit of the data in Figure 3 ($\Phi_N = 8.1kT$, $\Phi_A = 13.1kT$, and $\alpha_{NA} = 0.5$). This theoretical curve compares well with the data, which is an indication for the physical adequacy of the theoretical model. (Note that the data in Figure 3 are obtained at fixed c_{AT}, whereas the data in Figure 8a are obtained at fixed c_S). Figure 8b contains the calculated value of θ_A and θ_N, corresponding to the variation of σ in Figure 8a. With the increase of ξ, the Al^{3+} ions are replaced with Na^+ ions in order to satisfy eq 4.8; this affects the degrees of filling of the subsurface Stern layer with Al^{3+} and Na^+ counterions, θ_A and θ_N. One sees in Figure 8b that the adsorption of Al^{3+} ions strongly decreases, whereas the adsorption of Na^+ ions increases, approaching the value $\theta_N = 0.94$, which is comparable with the value determined for a solution without any Al^{3+} from Figure 6 above. Again, the greater adsorption energy of the Al^{3+} ions ($\Phi_A > \Phi_N$) leads to the fact that the decrease of θ_A (the desorption of Al^{3+} ions) causes an increase of σ with the increase of ξ (Figures 2 and 8a).

Finally, let us try to interpret the data for σ vs c_S in Figure 4, which correspond to a fixed value of ξ ($\xi = 1.07$). As already discussed, this case is the most difficult to be physically understood, and it is most probably affected by the competition of effects with opposite trends. The theoretical curve for σ vs c_S in Figure 4 is calculated by integrating eq 4.7 starting from the right-hand side experimental point as a boundary condition. This curve represents the best fit, corresponding to $\Phi_N = 8.4kT$, $\Phi_A = 10.0kT$, and $\alpha_{Na} = 0.5$, in spite of the fact that this time the agreement between theory and experiment is not so good. Nevertheless, the trend of the theoretical curve in Figure 4 is correct (increase of σ with the increase of the surfactant concentration c_S), and the calculated values of the bulk and surface ionic concentration allow one to judge which is the dominant factor determining this strange behavior of the plot of σ vs c_S. Figure 9a shows the calculated values of c_{NB} and c_{AB}, corresponding to the variation of σ in Figure 4. One sees that the increase of c_S leads to an increase of c_{AB} but decrease of c_{NB} (exactly the opposite to Figure 7a). This can be attributed to the fact that to increase c_S at fixed ξ, one has to increase proportionally c_{AT}; see eq 2.2. Then c_{AB} also increases, but not so rapidly, because of adsorption of a part of the Al^{3+} ions at the surface of the micelles. The linear increase of c_{AT} with c_S leads to a linear decrease of the sodium concentration (Figure 9a) because eq 4.8 (constancy of the ionic strength of the added electrolyte) is fulfilled in this experiment. Further, in Figure 9b, showing the calculated values of θ_A and θ_N, one sees that the degrees of filling of the subsurface Stern layer with Al^{3+} and Na^+ counterions are almost constant in this experiment, but θ_N is much larger than θ_A. The latter finding gives the key for understanding why the surface tension σ increases with the increase of the surfactant concentration c_S. The calculations show that the surfactant monomer concentration (CMC) does not change significantly in this case. On the other hand, the high degree of surface coverage with Na^+ ions, θ_N (see Figure 9b), makes the surface tension sensitive to the bulk concentration, c_{NB}, of Na^+; cf. eq 4.7. Thus the decrease of c_{NB} with the increase of c_S (Figure 9a) turns out to be the predominant factor determining the increase of σ with c_S in Figure 4; cf. eq 4.7.

Note, also, that there is no clear indication for the sphere-to-rod transition in the plot of σ vs c_S at *fixed* ξ; see Figure 4. Hence, the surface tension measurements can be used as an indicator for the sphere-to-rod transition in micelle shape if only a plot of σ vs ξ is available; see Figures 2 and 3.

For the time being we have observed an indication about the micellar sphere-to-rod transition in the plot of σ vs ξ with the anionic surfactant SDP-2S. One could expect a similar effect with other ethoxylated alkyl sulfates, such as SDP-1S, SDP-3S, etc., which is to be experimentally verified in the future.

5. Concluding Remarks

In this work we present experimental data showing that the surface tension, σ, of surfactant (SDP-2S) solutions undergoes a substantial change in the vicinity of the transition from sphere to cylinder in the micelle shape (the critical ratio); see Figures 2 and 3. The formation of cylindrical micelles at relatively low surfactant concentrations (between 2 and 8 mM) is promoted by the presence of Al^{3+} ions in the solution. In the experi-

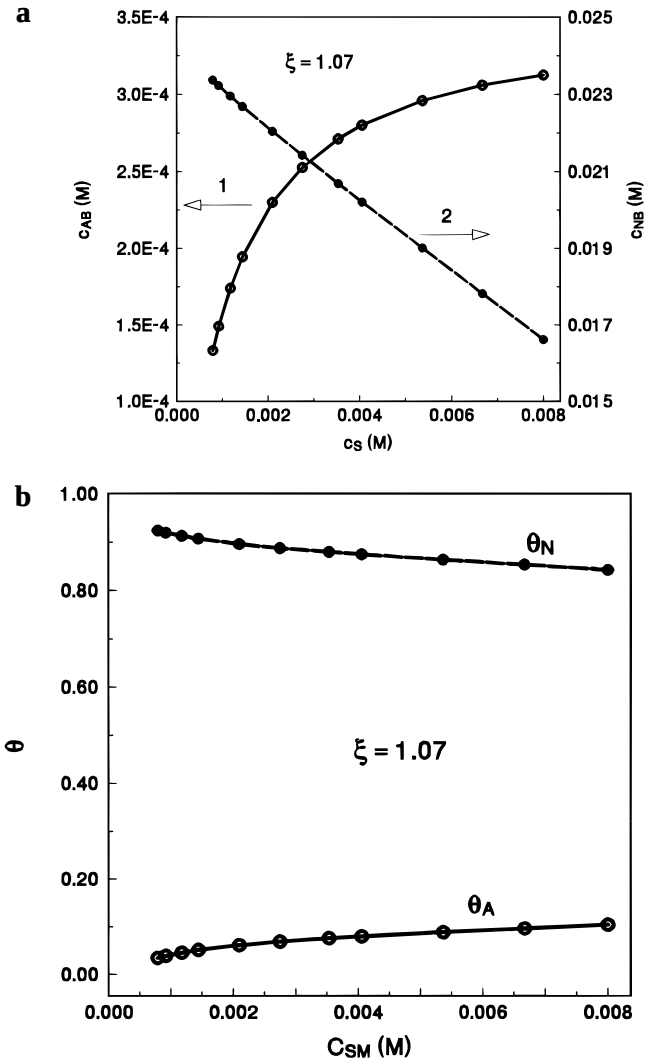

Figure 9. (a) Calculated values of c_{AB} (curve 1) and c_{NB} (curve 2) corresponding to the variation of the surface tension, σ, in Figure 4. The total surfactant concentration is constant, c_S = 0.008 M. (b) Calculated values of degrees of filling of the subsurface Stern layer with Al^{3+} and Na^+ counterions (cf. eq 4.5) corresponding to the variation of the surface tension, σ, in Figure 4. The parameter $\xi = 1.07$ is constant.

ments we fixed the ionic strength of the added electrolyte $I = 0.024$ M but varied the molar fractions of NaCl and $AlCl_3$.

We established that the observed variation of σ in the vicinity of the critical ratio can be attributed to two competitive effects: (i) competition between Na^+ and Al^{3+} counterions for the adsorption in the subsurface Stern layer and (ii) competition between the solution surface and the surfaces of the micelles to adsorb the multivalent Al^{3+} counterions. The situation is additionally complicated by the fact that the concentration of Al^{3+} is comparable with the surfactant concentration, and consequently, the concentration of free Al^{3+} might be substantially reduced due to binding of Al^{3+} to the micelles. The latter effect was studied experimentally by means of the ultrafiltration experiments; see Figure 5.

To account for the binding of Al^{3+} to the micelles, we develop a theoretical model based on eqs 3.9 and 3.10, which allows us to calculate the true bulk (background) concentrations of Na^+ and Al^{3+} ions, c_{NB} and c_{AB}, as well as the true ionic strength of the solution, I_t; see eq 3.2.

Further, we describe the variation of the surface tension, σ, based on the Gibbs adsorption equation, eq 4.7, combined with Langmuir type adsorption isotherms for the Na^+ and Al^{3+} ions, eq 4.5. The theory agrees well with the experiment; see Figures 3 and 8a. The observed variation of the surface tension in the vicinity of the critical ratio is due to the exchange of the Al^{3+} ions with Na^+ ions in the subsurface Stern layer of the solution: see Figures 7b and 8b.

The calculations show that the degree of filling of the Stern layer with Na^+ ions is relatively high and can reach 86% in the absence of the competitive Al^{3+} ions; see Figure 6 and the discussion after it. This makes the surface tension of solution sensitive to the bulk concentration of Na^+. Thus it may happen that the surface tension increases when the total surfactant concentration increases, because of a decrease in the bulk Na^+ concentration; see Figures 4 and 9a,b.

In summary, the present work shows that the transition from sphere to cylinder in the micelle shape in the presence of Al^{3+} counterions can be detected by surface tension measurement (at least for the investigated surfactant solutions). The transition appears as a sharp change of the surface tension plotted vs the surfactant to Al^{3+} ratio; see Figures 2 and 3. The paper contains also experimental data for the dependence of the CMC and surface tension of SDP-2S on the ionic strength (eq 2.1 and Figures 1 and 6), which may represent independent interest.

Acknowledgment. This work was supported by Colgate-Palmolive and by the Bulgarian National Science Fund. The authors are indebted to Dr. D. Petsev for his stimulating interest in this study and to Mrs. E. Basheva for measuring part of the experimental points in Figure 6.

Appendix: Procedure of Calculations

The goal of the procedure of calculations is to fit the experimental data (a) for the surface tension σ vs ξ at fixed total Al concentration, c_{AT} (Figure 3); (b) for the surface tension σ vs ξ at fixed total surfactant concentration, c_S (Figures 2, 8a); and (c) for the surface tension σ vs c_S at fixed surfactant-to-Al ratio, ξ (Figure 4).

1. *Input parameters:* the total surfactant concentration, c_S; the total Al concentration, c_{AT}; the apparent ionic strength of the added electrolyte, $I \equiv 0.024$ M; the surfactant adsorption, $\Gamma_S \equiv 2 \times 10^{14}$ cm^{-2}. In addition, $H_1 = 1.64$ mM and $H_2 = 0.407$ mM (see eq 3.11); ξ and c_{SM} are calculated from eq 2.2, where the CMC is determined from eq 2.1 with the above value of I. In case (c) ξ is an input parameter. The total Na^+ concentration, c_{NT}, is calculated from eq 4.8.

2. Trial values of c_{AB} and α_{Na} are assumed. Then α is calculated from eq 3.10. The true ionic strength, I_t, and CMC are calculated by solving together eqs 3.3 and 2.1 (the latter with $I = I_t$). Then c_{AB} is determined by solving numerically eq 3.9. The background Na^+ concentration, c_{NB}, is calculated from eq 3.1. Thus CMC, c_{NB}, and c_{AB} are determined as functions of ξ and c_S.

3. Next, eq 4.7 is integrated numerically. In cases (a) and (b) CMC, c_{NB}, and c_{AB} are supposed to be functions of ξ, calculated as explained in point 2 above. Likewise, in case (c) CMC, c_{NB} and c_{AB} are supposed to be functions of c_S calculated in the same way, but at constant ξ. θ_A, θ_N, b_A, and b_N are calculated from eqs 4.5 and 4.6.

4. The calculated curve for σ vs ξ (or σ vs c_S) is then compared with the experimental points in Figures 2, 3, 4, or 8a, and the adjustable parameters Φ_A, Φ_N, and α_{Na} are determined by means of the least squares method.

LA970399D